Detection of Explosive Markers Using Zeolite Modified Gas Sensors†

William J. Peveler,[a] Russell Binions,[b], Stephen M.V. Hailes,[c] and Ivan P. Parkin*[d]

Received Xth XXXXXXXXXX 20XX, Accepted Xth XXXXXXXXX 20XX
First published on the web Xth XXXXXXXXXX 200X
DOI: 10.1039/b000000x

Detection of hidden explosive devices is a key priority for security and defence personnel around the globe. Electronic noses, based on metal oxide semiconductors (MOS), are a promising technology for creating inexpensive, portable and sensitive devices for such a purpose. An array of seven MOS gas sensors was fabricated by screen printing, based on WO_3 and In_2O_3 inks. The sensors were tested against six gases, including four explosive markers: nitromethane, DMNB (2,3-dimetheyl-2,3-dinitrobutane), 2-ethylhexanol and ammonia. The gases were successfully detected with good sensitivity and selectivity from the array. Sensitivity was improved by overlaying or admixing the oxides with two zeolites, H-ZSM-5 and TS-1, and each showed improved responses to -NO_2 and -OH moieties respectively. Admixtures in particular showed promise, with excellent sensitivity and good stability to humidity. Machine learning techniques were applied to a subset of the data and could accurately classify the gases detected, even when confounding factors were introduced.

1 Introduction

Explosives are the primary tool of terrorists in the world. In the period 2009-2011, improvised explosive devices (IEDs) were consistently responsible for over 50% of coalition deaths in Operation Enduring Freedom, Afghanistan.[1,2] Key threats include car bombs, suicide bombs and other IEDs, as well as mines and unexploded munitions from previous conflicts.

Many methods for the detection of explosives exist, and bulk detection methods (x-ray, terrahertz or neutron absorption) are routinely used in ports and airports. However, vapour detection is also a useful tool. It allows high-throughput, non-invasive detection of a range of chemicals, without having to subject every person or object to close individual scrutiny. It can also provide information on the types of material detected to allow rapid assessment of the threat level.

There are many different methods to detect explosive vapour in current development, such as Ion Mobility Spectrometry (IMS) and fluorescent polymers, and the "gold standard" - the sniffer dog - is still favoured.[3–9] However these detectors are expensive to run and maintain, for example a canine for explosives detection costs up to $6,000 to train and $2,000 p.a. to maintain, in addition to the cost of a trained and dedicated handler.[10]

Metal oxide semiconducting gas sensors (MOS sensors) are a low cost and increasingly reliable form of vapour detector. Their ease of production and small size gives them great potential for a commercial explosives detector; however, they often lack the crucial sensitivity and selectivity to detect low vapour pressure materials such as RDX (1,3,5-trinitro-1,3,5-triazacyclohexane) or TNT (2,4,6-trinitrotoluene).[11,12]

In recent years a lot of attention has been paid to the use of filtering or transformational elements, overlaid on the metal oxide to improve sensitivity and selectivity. These elements filter the gas that reaches the sensing oxide by size and molecular structure. One set of very successful materials for this purpose have been zeolites, which act simultaneously as both filter and catalyst.[13–17].

To gain maximum selectivity from these sensors it is necessary to incorporate them into an electronic nose (e-nose).[18–22] Sensors are varied by material, coatings or temperature and measurements from each sensor, such as the change in resistance, the speed of response, or functions thereof (for example linear combinations), can be used to create a fingerprint of an analyte. Even the position in an array can add discriminatory effects.[20,23] The data collected can be processed with multivariate clustering techniques, such as principal component analysis, or classifying techniques, such as neural networks and support vector machines (SVMs).[24–30]

The aim of this study was to develop an array of MOS sensors to detect a set explosive marker gases and develop an automated classification of gases detected. This is the first step towards a prototype portable e-nose for explosives. It is

[a] *Dept. of Security and Crime Science, University College London, 35 Tavistock Sq., London, UK, WC1H 9EZ*
[b] *School of Engineering and Materials Science, Queen Mary University of London, Mile End Road, London, UK, E1 4NS*
[c] *Dept. of Computer Science, University College London, Gower St., London, UK, WC1E 6BT*
[d] *Dept. of Chemistry, University College London, 20 Gordon St., London, UK, WC1H 0AJ Fax: +44 (0)20 7679 7463; Tel: +44 (0)20 7679 4669; E-mail: i.p.parkin@ucl.ac.uk*
† Electronic Supplementary Information (ESI) available: See DOI: 10.1039/b000000x/

the first time zeolitic overlayers on indium oxide sensors have been studied, and the first testing of MOS sensors against several of the marker gases. The methodology is presented, followed by analysis and discussion of the sensor properties and gas testing results, as well as the machine-learning techniques used for classification.

2 Materials and Methods

2.1 Material and analyte selection

Two n-type metal oxides were used: tungsten trioxide (WO_3) for its efficacy in detecting NO_2 and other oxidising gases[19,31–34], and indium oxide (In_2O_3) for detection of peroxides and other explosive gases.[35–39] Overlayers and admixtures were created using two types of zeolite, H-Zeolite Socony Mobil (ZSM)-5 and Titanium Silicate (TS)-1. H-ZSM-5 has been shown to improve sensitivity of WO_3 sensors to NO_2, so it was anticipated that it may do the same for molecules containing an -NO_2 group.[34] TS-1 was used for the first time, in an attempt to improve sensitivity to alcohols and peroxides.[40,41] Both zeolites have an MFI type microporous structure, with Al^{3+} centres in the H-ZSM-5 replaced by Ti^{4+} in TS-1. The micropore size of H-ZSM-5 is around 5.5 Å, and TS-1 has an expanded structure due to the larger titanium ion, giving slightly larger micropores.[42,43]

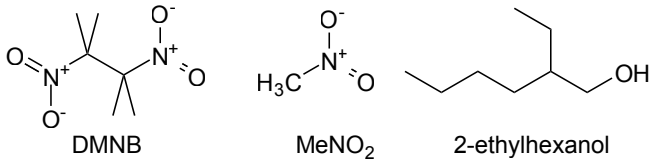

Fig. 1 Molecular structures of three of the six analytes used in this study

Seven types of sensor were synthesised, and trialled against six gases: $MeNO_2$ is explosive in its own right, but has also been used as an additive in ammonium-nitrate/fuel-oil (ANFO) explosives by terrorists.[44] Few studies have previously examined MOS gas sensing of $MeNO_2$.[45,46] DMNB (2,3-dimethyl-2,3-dinitrobutane - Fig. 1) is used as a taggant in military explosive to assist with detection and is another example of an aliphatic nitro-alkane, with a more complex alkyl backbone.[47] NO_2 is a strong oxidant and toxic atmospheric pollutant, and was included as a comparison to the aliphatic nitro-compounds.[19,31,32,34] The two alcohols were 2-ethylhexanol, a long-chain alcohol which occurs as a plasticiser in *C4* plastic explosive formulation and other explosives,[10] and ethanol, included as a comparison. Finally, ammonia was included, as a potential indicator of home-made explosives concocted from cleaning products.[48]

Table 1 Table of sensors produced with abbreviated names. Bracketed numbers indicate the number of layers printed. "In" indicates the metal oxide is In_2O_3, "W" indicates WO_3. A '+' indicates an admixture of metal oxide and zeolite, and a '.' an overlayer of zeolite upon metal oxide. The numbers correspond to the number of layers deposited where applicable

Sensor	Metal Oxide	Overlay
W.5	WO_3(5)	nil
In.5	In_2O_3 (5)	nil
W.5.TS1.2	WO_3 (5)	TS-1 (2)
In.5.TS1.2	In_2O_3 (5)	TS-1 (2)
In.5.ZSM.2	In_2O_3 (5)	H-ZSM-5 (2)
In+TS1.5	In_2O_3, 30% TS-1 (5)	nil
In+ZSM.5	In_2O_3, 30% H-ZSM-5 (5)	nil

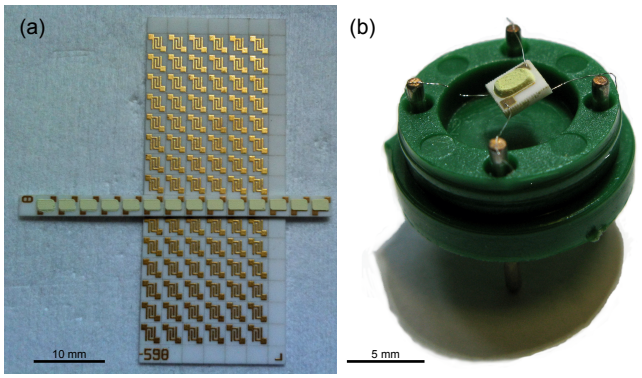

Fig. 2 (a) A half sheet of unprinted 3x3 mm sensing chips and a printed 14 sensor strip. (b) Bonded WO_3 sensor.

2.2 Sensor fabrication

Seven types of sensor were produced for the array using In_2O_3 and WO_3 powders, and H-ZSM-5 and TS-1 zeolites. All sensors were produced by screen printing metal oxide inks onto 3×3 mm alumina substrate tiles, containing laser etched gold electrodes and an integrated platinum heater track. The inks were produced by mixing the metal oxide with an organic vehicle (ESL-400, Agmet. Ltd). Overlayers were created by mixing the zeolites with vehicle in a similar fashion, and admixtures incorporated zeolites (30% by mass), with the metal oxide ink (Table 1). The inks were ground by pestle and mortar to give a smooth, homogeneous suspension. Screen printing was performed using a DEK1202, printing each layer onto a strip of 14 alumina substrate tiles simultaneously (Fig. 2a). Between each application, the previous layer was dried for 10 minutes under an infra-red lamp. Five layers of metal oxide were printed for each sensor, overlayered with two zeolite layers where applicable. The strip was separated into individual

sensors, and calcined in a furnace at 600°C for one hour. This burnt off the organic vehicle and sintered the sensing element to the substrate. Side-on scanning electron microscopy (SEM) measurements suggested a thickness of ca. 75 μm.

The sensors were bonded onto brass pins in a standard polyphenylene sulphide housing (Fig. 2b); using platinum wire and a MacGregor DC601 parallel gap resistance welder.

Metal oxides for the inks were used as supplied by Sigma Aldrich. TS-1 zeolite was produced from a synthesis described by Uguina et al.[49] H-ZSM-5 zeolite was produced by firing a sample of NH_4-ZSM-5 at 100°C for 8 hours to remove moisture, before ramping the temperature to 500°C for a further 12 hours to remove ammonia.

2.3 Characterisation techniques

The sensors were subject to characterisation by X-ray Diffraction (XRD), Scanning Electron Micrsocopy (SEM) and Energy Dispersive X-ray (EDX) spectroscopy. XRD data were collected over the 2θ range 10° to 65°, with step size 0.02°, on a Brucker GADDS D8 diffractometer using Cu K_α radiation (λ = 0.15418 nm). Powder patterns of the zeolites were collected on a Brucker D4 powder diffractometer over the 2θ range 5° to 65°, with step size 0.05°.

Scanning electron micrographs were collected on a Jeol JSM-6301F microscope, in secondary electron imaging mode, using a 5 keV probe voltage. The images were digitally recorded in SemAfore software and noise removal and resizing was performed in Photoshop Elements 8.

EDX analysis was performed using a 20 keV SEM probe coupled with an Oxford Instruments INCA X-Sight system and associated software and confirmed the atomic percentage make up of each sample.

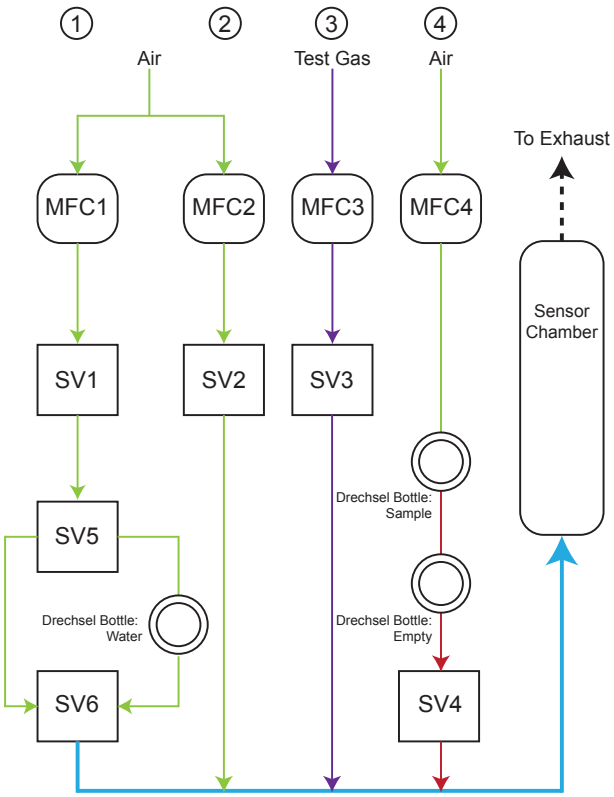

Fig. 3 Flow diagram apparatus, with channels indicated by the circled numbers. Channel 1 produces wet air, channel 2 dry air, channel 3 cylinder gas and channel 4 samples headspace of liquids and solids in the Drechsel bottle. Mass-flow controllers (MFCs) and solenoid valves (SVs) 1-4 are located on their respective channels. SVs 5 and 6 control the proportion of humidity. The empty Drechsel bottle buffers air flow over the sample, ensuring a more constant concentration.

2.4 Gas testing system and protocol

The experimental setup used for testing the array is shown in Fig. 3 and consists of a sensor chamber, with gas flow controlled by mass-flow controllers. A potential divider circuit and analog to digital converter card facilitated recording of the sensors' resistance. The sensors' integrated Pt heater tracks were set to 350, 400 or 500 °C using separate, potentiostat-controlled, DC voltage circuitry. Dry air was used as a purge and carrier gas, but humidity could be introduced *via* a humidifier loop. Variable concentrations of test gas were introduced into a fixed flow of 1000 cm^3 min^{-1}. Gases were used at a proportion between 5 and 50% of their cylinder concentration or vapour pressure, to test the lowest possible concentrations that could be generated by the apparatus. NO_2 (1 ppm), NH_3 (50 ppm) and EtOH (100 ppm) were from BOC supplied cylinders. DMNB (3 ppm), $MeNO_2$ (5000 ppm) and 2-ethylhexanol (296 ppm) were generated by passing air over a sample of the analyte. Vapour pressures were approximated at 25 °C and 1 atm.[1]

The sensitivity of the sensors was measured as a function of their base-line resistance in air. The resistance of each sensor was measured just before the test gas was introduced to the sensor chamber (R_0), and during test gas flow (R). The sensor response, S, was defined as $S = R/R_0$ for oxidising gases and R_0/R for reducing gases. The difference in S just before a gas pulse, defined S_0, and the maximal value of S during a gas pulse, S_{max}, was calculated to find the magnitude of sensor response from the base-line, $|S| = S_{max} - S_0$.

The seven sensors in the chamber were allowed to equilibrate for 30 minutes at the selected temperature, in a flow of dry air, to measure R_0. They were then exposed to 600 s pulses of each test gas at varying concentrations, with a 900 s air purge between each pulse. Further experiments collected data at 50% humidity and with shorter and longer pulse lengths

(150 s, 300 s and 900 s). If humidity was used, then the base-line was allowed to re-equilibrate for an additional 900 s before the next gas pulse. The response magnitude measurement $|S|$ was used in construction of a Support Vector Machine (SVM) to analyse and classify the data.

3 Results and Discussion

3.1 Sensor material characterisation

Seven types of sensor were produced using a screen printing technique followed by calcination, using In_2O_3 and WO_3 powders, and H-ZSM-5 and TS-1 zeolites. These are described in Table 1, and include sensors comprised of an overlayer of zeolite on top of a metal oxide layer, and admixed sensors where the single layer contains a mix of metal oxide and zeolite.

XRD patterns were collected for each sensor and powder samples of ZSM-5 and TS-1 zeolite (Fig. 4). These patterns confirmed that WO_3 and In_2O_3 composition were unchanged by calcination or by heating and gas testing, and that the zeolitic materials were unchanged by incorporation into the sensors. The only oddity is the appearance of indium oxide peaks through the zeolitic overlayer in In.5.ZSM.2. This is likely due to a slightly thinner film at the point of sampling.

SEM micrographs are given in Fig. 5 at around 10,000x magnification. Visual inspection showed the porous nature of the metal oxide or zeolite surfaces, with a variety of particle sizes evident. Pure tungsten oxide exhibits platelet-like structures of circa 1 μm at its surface (Fig. 5a). The pure indium oxide sensor shows a cubic habit with a large range of grain sizes, ranging from 100 nm to 1 μm (Fig. 5b). The appearance of TS-1 zeolite is consistent in each sensor it was used on, and characterised by its large spherical grains of diameter 2 μm interspersed with large plate-like particles (Fig. 5c + 5d). H-ZSM-5 zeolite has a substantially different structure, consisting of smaller, berry-like clusters, around 200 nm in diameter (Fig. 5e). On admixing with In_2O_3, they appear to have segregated to the top of the sample, with few cubic oxide particles visible (Fig. 5g). This difference in appearance suggests that the small H-ZSM-5 particles will have a larger total surface area, in comparison to the larger TS-1 particles, but the range of sizes present in the TS-1 leads to great porosity in the zeolite overlayer.

EDX analysis shows the atom types present are as expected, with trace impurities - both types of zeolite showed trace potassium (<0.3 atomic percent). From an average of all the measurements taken of TS-1 zeolite, on both fired and un-fired samples, a titanium incorporation of circa 0.95% was calculated. The same calculation for H-ZSM-5 showed the Si:Al ratio to be around 50:1. No trace of N (indicating residual ammonia) was visible in the EDX spectrum of the H-ZSM-5.

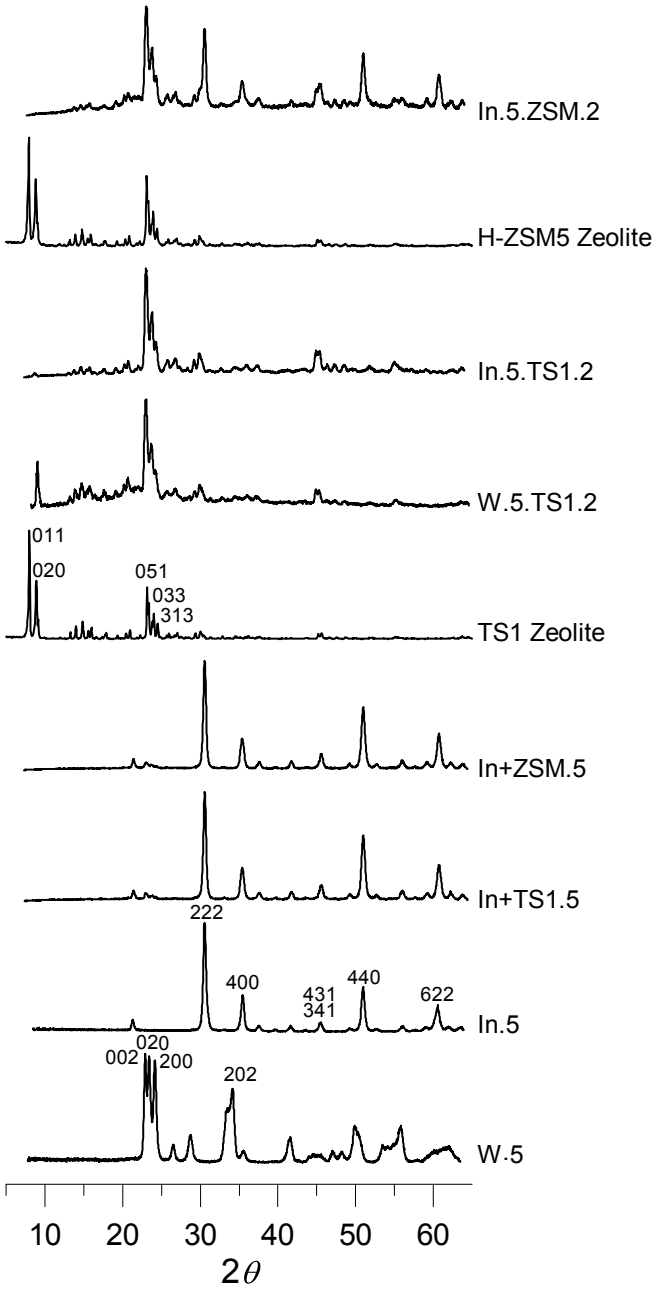

Fig. 4 XRD spectra for all sensors and pure samples of each overlayer zeolite, collected between circa 5° and 65°. The y-axis is normalised and offset for each spectrum. Sensor namings are given in Table 1. The principal peaks are indexed according to standards from the literature.[34,39,50]

3.2 Gas sensitivity testing

All gases tested, with the exception of NO_2 were reducing, and thus the resistance of the sensors decreased on exposure

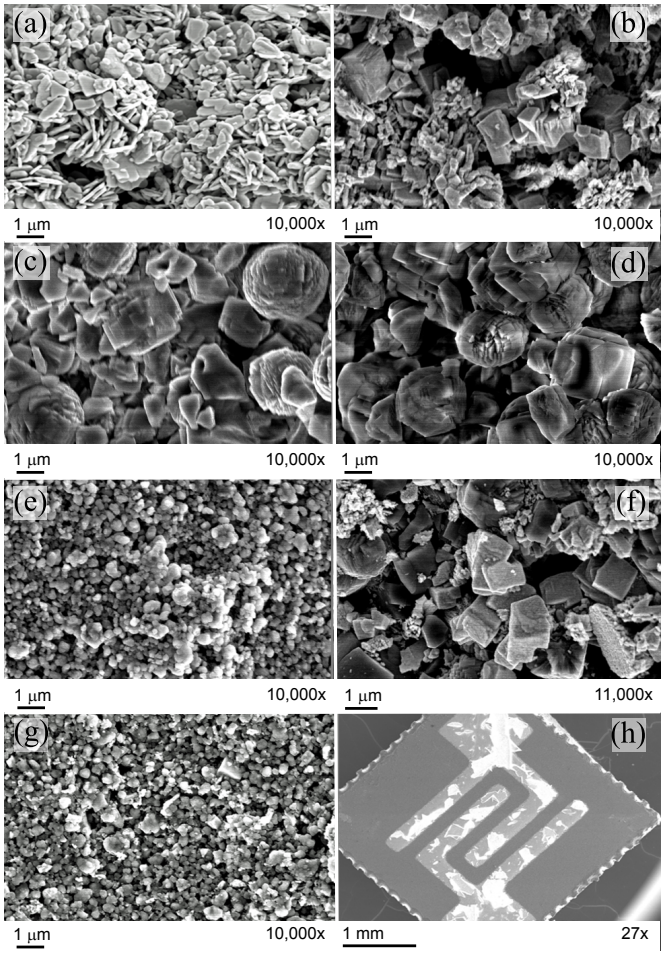

Fig. 5 SEM micrographs for each sensor produced and a blank chip. All imaged at 10k× magnification unless noted: a) W.5 b) In.5 c) W.5.TS1.2 d) In.5.TS1.2 e) In.5.ZSM.2 f) In+TS1.5 (11k×) g) In+ZSM.5 h) Blank sensor substrate (27×)

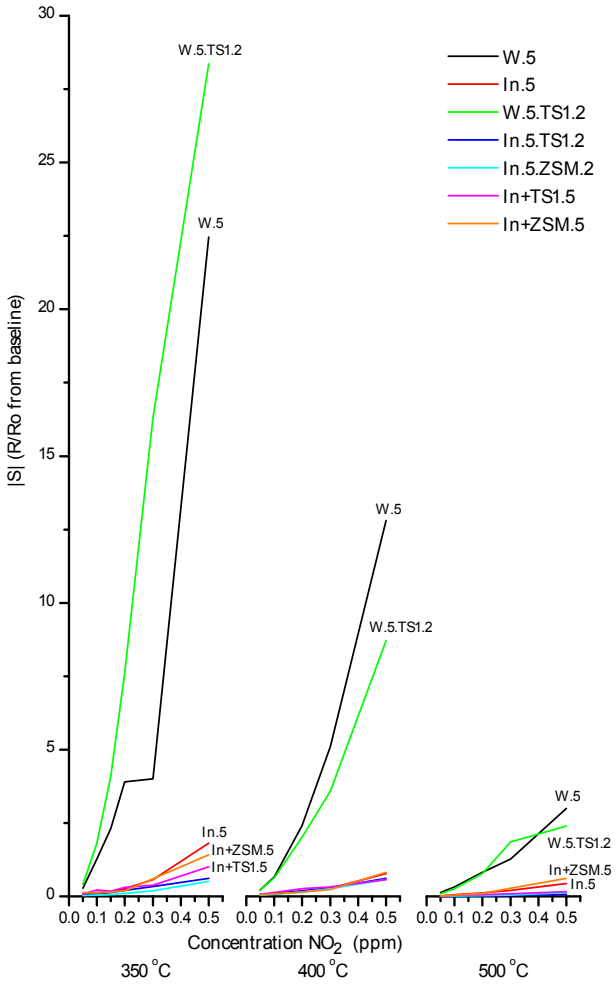

Fig. 6 Sensor responses to NO_2 concentrations between 0.05 and 0.5 ppm, at 350, 400 and 500 °C in dry air for a 600 s exposure. The most responsive sensors (not all) are labelled for clarity.

to the gas. The sensors were usually most sensitive to the gases at the lowest temperature of 350 °C and sensitivity decreased with increasing temperature. There were a few key exceptions to this trend, particularly for NH_3 and EtOH.

For NO_2 the WO_3 sensors performed best, with the transformational TS-1 zeolite overlayer conferring a degree of extra sensitivity at lower temperatures (Fig. 6). At higher temperatures the Knudsen diffusion of gas molecules though the zeolite pores becomes slower, due to a greater number of collisions with the pore walls, and so sensitivity falls.[51] This effect is less pronounced for the uncoated WO_3 sensor, due to its more open structure. In_2O_3 based sensors gave a much lower sensitivity at all temperatures but, of those, plain In.5 and In+ZSM.5 gave the best sensitivity.

The best sensitivity to $MeNO_2$ was achieved by In_2O_3 admixed with H-ZSM-5 zeolite (In+ZSM.5). At the lowest temperature, overlaying with zeolites also imparted enhanced sensitivity. However, as for the case above, this enhancement fell away with increasing temperature due to the Knudsen diffusion effect.

Although sensitivity to NH_3 was low, the most promising sensor was In.5, at 350 °C. As the temperature increased, an inversion of trend occurred, with W.5 and W.5.TS1.2 responses becoming far stronger than those for In_2O_3 at 400 and 500 °C. A similar inversion took place for EtOH. At the lowest temperature In.5 was again the most responsive sensor, but as temperature increased, In+TS1.5 started to show a stronger response (Fig. 7). TS-1 zeolite is known to catalyse the oxidation of alcohols, using the Lewis acidic Ti sites and a source of oxygen (such as peroxide or the air), and thus it is suggested that increasing the temperature favours this reaction

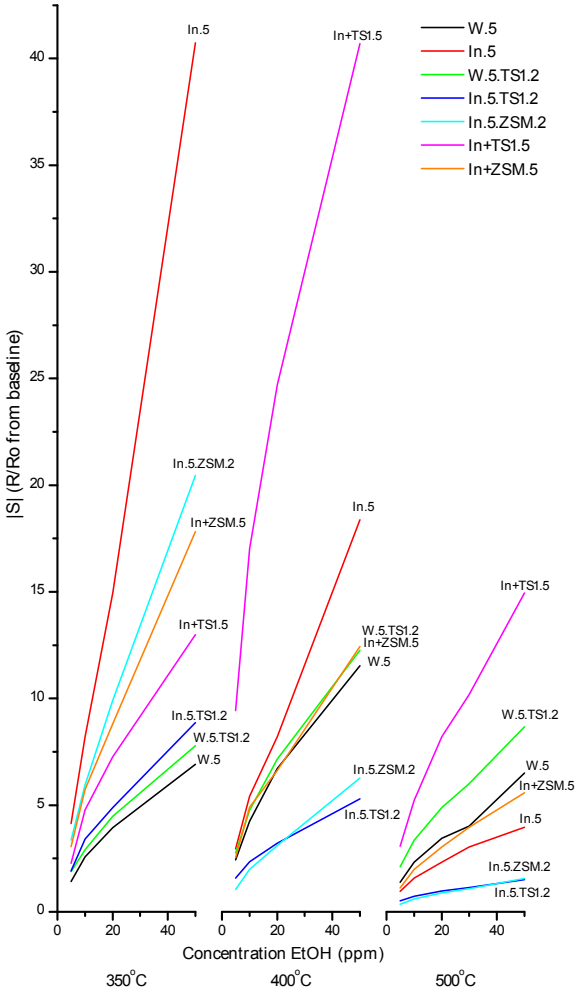

Fig. 7 Sensor responses to EtOH concentrations between 5 and 50 ppm, at 350, 400 and 500 °C in dry air for a 600 s exposure.

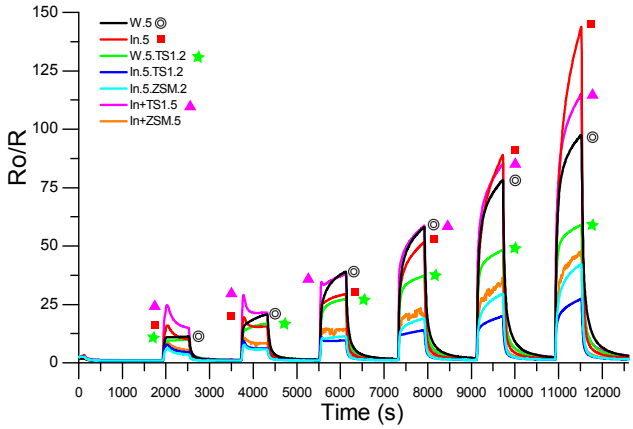

Fig. 8 Response peaks for 7 sensors exposed to 600 s pulses of 2-ethylhexanol. Concentrations were circa 15, 30, 59, 89, 118, and 148 ppm in dry air and the sensors were heated to 400 °C. For clarity in monochrome, the four most responsive sensors are indicated (at each maximal Ro/R) with a symbol, as given in the key.

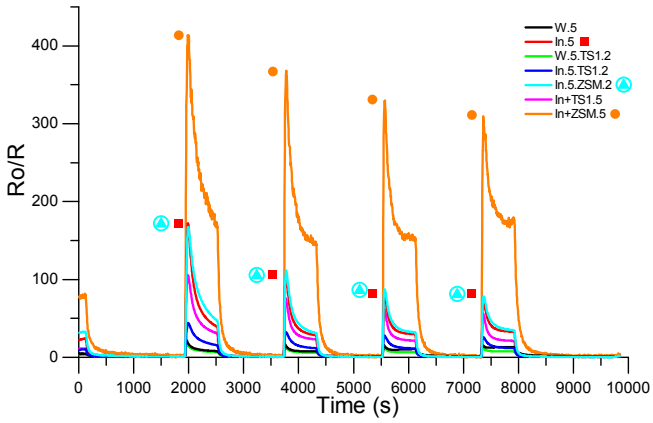

Fig. 9 Response graph for 7 sensors exposed to 600 s pulses of four concentrations (starting at circa 1.5 ppm) of DMNB at 350 °C in dry air. For clarity in monochrome, the three most responsive sensors are indicated (at each maximal Ro/R) with a symbol, as given in the key.

pathway.[40]

Two of the gases underwent multiple reactions on the sensor surface, causing an initial and secondary sensing response. This occurred for both DMNB and 2-ethylhexanol, where an initial strong response dropped off quickly to a lower value for the remainder of the gas pulse (Fig. 8 and 9). In_2O_3 based sensors were particularly affected by this, but still had high sensitivity to the gas. For 2-ethylhexanol, the WO_3 sensors gave a low, but typical response for every concentration tested, whereas the In_2O_3 sensors gave the malformed response at lower concentrations which became more typical at higher concentrations (Fig. 8). This suggests that at higher concentrations one of the multiple surface reactions begins to dominate, giving a single, typical sensor response.

The most sensitive element to DMNB was In+ZSM.5, but there was no increase in response on increasing concentration, due to the set-up of the headspace sampling apparatus, with the full headspace concentration taking longer to re-establish than the time between gas pulses (Fig. 9). It is interesting to note that the admixed In+ZSM.5 sensor performed well for each -NO_2 containing molecule tested, attributable to the catalytic response. For 2-ethylhexanol at low concentrations, In+TS1.5 was promising (in line with the predictions in Section 2.1), but In.5 and W.5 had greater responses at the higher concentrations.

Of all the sensors, the admixed metal oxides and zeolites seemed to give a good balance of enhanced sensitivity and selectivity, overcoming the high-temperature diffusion issues

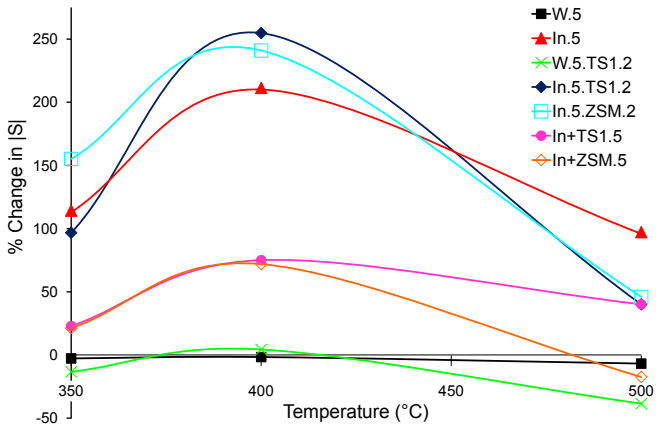

Fig. 10 Average percentage change in sensor response on exposure to 50% humidity at 350, 400 and 500 °C

with overlayered sensors, and increasing the porosity of the microstructure, thus enhancing responses more generally.

3.3 Humidity effects

Sensor response was measured for four of the gases at 10% of their full concentration, over a 600 s gas pulse at 0% or 50% humidity. Almost all the sensors showed a change in response under the more humid conditions. Average percentage change from $|S|$ at 0% humidity was calculated for each sensor over NO_2, $MeNO_2$, NH_3 and EtOH, and is plotted in Fig. 10 against temperature. The sensitivity to humidity was greater at 400 °C than either 350 or 500 °C. This change was most marked for plain indium oxide and overlayed indium oxide sensors, showing poor humidity tolerance with a >100% change in response below 500 °C. The large difference between different temperatures is hypothesised to be due to the rate of diffusion of moisture through the overlayer. Admixed indium oxide sensors showed a reasonably small percentage change at each temperature, and tungsten oxide sensors showed almost no change in response to humidity at any of the temperatures investigated.

How much this variation in data effects the possibility of classifying the data was investigated using machine learning techniques.

3.4 Training of a classification algorithm

A support vector machine (SVM) was applied to a subset of the data. The SVM was constructed using data from four of the six gases, NO_2, $MeNO_2$, NH_3 and EtOH. A full background to SVMs and explicit details of the model constructed for this work are available in the Electronic Supporting Information (ESI).

The SVM showed excellent classification ability when tested on the array data, with greater than 85% accuracy even when confounding factors such as humidity or variable gas exposure times were introduced. When the SVM was tested using data collected for a set gas pulse length (600s) and at 0% humidity, a classification accuracy of 85.92% was achieved. If the SVM was tested against data collected at 50% humidity the accuracy fell to 85.00%; however when data collected at variable gas pulse lengths were analysed by the SVM, an accuracy of 89.77% was achieved.

The application of an SVM to the data set proved very successful. Of the four gases included, NO_2 was readily recognised due to its oxidising response, particularly on normalisation of the data. NH_3 and EtOH were the most confused, due to their more similar reducing responses. The algorithm was capable of reasonable evaluation of gas type, even when concentration data was not available, and confounding factors such as changing humidity and variable gas pulse length were introduced. It should be possible to increase classification accuracy by the design of a more varied sensor array, using additional metal oxides and transformational elements. The inclusion of a p-type metal oxide would be especially useful in determining whether a detected gas was oxidising or reducing.

4 Conclusions

A sensor array of seven thick-film MOS sensors was produced using just two basic metal oxides and two zeolites;

1. It included the first recorded use of zeolites in conjunction with In_2O_3 for gas sensing. These sensors were particularly selective towards reducing gases, although some showed poor stability to humidity.

2. The array also included the first use of TS-1 zeolite for gas sensing purposes. This material improved sensitivity and selectivity to alcohols, especially at high temperatures, and is anticipated to also work well for the detection of peroxide materials.

3. Admixed materials containing a metal oxide and zeolite showed improved sensitivity and selectivity due to a combination of open microstructure and catalytic influence of the zeolites.

4. H-ZSM-5 zeolite has been shown to improve sensor responses to nitro-group containing materials - particularly relevant for the detection of explosives.

5. WO_3 had good stability to humidity, and as previously reported, was very sensitive to oxidising NO_2 gas.

6. All the results were subjected to classification with a machine-learning tool, and high levels of accuracy were reached (>85%), even when confounding elements were introduced, such as humidity.

This system has great promise for application in the detection of explosives or explosive markers, and shows the promise of e-noses based on MOS technology.

5 Acknowledgments

Steve Firth, Kevin MacDonald, Martin Vickers and Len Parrish are thanked for their help with the instrumentation. This work was carried out under EPSRC Grant no: EP/G037264/1 as part of UCL's Security Science Doctoral Training Centre.

References

1 M. Marshall and J. C. Oxley, *Aspects of Explosive Detection*, Elsevier, Oxford, 2009, ch. 1-2, pp. 1–26.
2 www.iCasualties.org, *Data on deaths for Operation Enduring Freedom*, 2009-2011, www.icasualties.org.
3 G. Eiceman and H. Schmidt, *Aspects of Explosives Detection*, Elsevier, Oxford, 2009, ch. 9, pp. 171–202.
4 G. A. Eiceman and J. A. Stone, *Analytical Chemistry*, 2004, **76**, 390 A–397 A.
5 J.-S. Yang and T. M. Swager, *Journal of the American Chemical Society*, 1998, **120**, 11864–11873.
6 J.-S. Yang and T. M. Swager, *Journal of the American Chemical Society*, 1998, **120**, 5321–5322.
7 T. M. Swager, *Accounts of Chemical Research*, 1998, **31**, 201–207.
8 J. Yinon, *Analytical Chemistry*, 2003, **75**, 98 A–105 A.
9 R. J. Harper, J. R. Almirall and K. G. Furton, *Talanta*, 2005, **67**, 313–327.
10 K. G. Furton and L. J. Myers, *Talanta*, 2001, **54**, 487–500.
11 K. Brudzewski, S. Osowski and W. Pawlowski, *Sensors and Actuators B: Chemical*, 2012, **161**, 528–533.
12 Y. Gui, C. Xie, J. Xu and G. Wang, *Journal of Hazardous Materials*, 2009, **164**, 1030–1035.
13 D. Mann, K. Pratt, T. Paraskeva, I. Parkin and D. Williams, *Sensors Journal, IEEE*, 2007, **7**, 551–556.
14 D. P. Mann, T. Paraskeva, K. F. E. Pratt, I. P. Parkin and D. E. Williams, *Measurement Science and Technology*, 2005, **16**, 1193.
15 A. Afonja, R. Binions, S. Dungey, I. Parkin, D. Lewis and D. Williams, *Procedia Engineering*, 2010, **5**, 103–106.
16 R. Binions, H. Davies, A. Afonja, S. Dungey, D. Lewis, D. E. Williams and I. P. Parkin, *Journal of The Electrochemical Society*, 2009, **156**, J46–J51.
17 R. Binions, A. Afonja, S. Dungey, D. W. Lewis, I. P. Parkin and D. E. Williams, *Sensors Journal, IEEE*, 2011, **11**, 1145–1151.
18 A. Berna, *Sensors*, 2010, **10**, 3882–3910.
19 A. A. Tomchenko, G. P. Harmer, B. T. Marquis and J. W. Allen, *Sensors and Actuators B: Chemical*, 2003, **93**, 126–134.
20 F. Rock, N. Barsan and U. Weimar, *AIP Conference Proceedings*, 2009, **1137**, 140–143.
21 Z. Haddi, F. Annanouch, A. Amari, A. Hadoune, B. Bouchikhi and N. El-Bari, *IEEE Sensors*, 2010, 771–774.
22 S. S. Chowdhury, B. Tudu, R. Bandyopadhyay and N. Bhattacharyya, *IEEE Region 10 and the Third international Conference on Industrial and Information Systems*, 2008, 1–5.
23 F. K. Che Harun, J. E. Taylor, J. A. Covington and J. W. Gardner, *Sensors and Actuators B: Chemical*, 2009, **141**, 134–140.
24 M. K. Muezzinoglu, A. Vergara, R. Huerta, N. Rulkov, M. I. Rabinovich, A. Selverston and H. D. I. Abarbanel, *Sensors and Actuators B: Chemical*, 2009, **137**, 507–512.
25 A. Z. Berna, A. Vergara, M. Trincavelli, R. Huerta, A. Afonja, I. P. Parkin, R. Binions and S. Trowell, *AIP Conference Proceedings*, 2011, **1362**, 50–52.
26 A. Z. Berna, A. R. Anderson and S. C. Trowell, *PLoS ONE*, 2009, **4**, e6406.
27 N. El Barbri, A. Amari, M. Vinaixa, B. Bouchikhi, X. Correig and E. Llobet, *Sensors and Actuators B: Chemical*, 2007, **128**, 235–244.
28 J. W. Gardner, H. W. Shin and E. L. Hines, *Sensors and Actuators B: Chemical*, 2000, **70**, 19–24.
29 A. Amari, N. El Barbri, E. Llobet, N. El Bari, X. Correig and B. Bouchikhi, *Sensors*, 2006, **6**, 1209–1223.
30 N. El Barbri, E. Llobet, N. El Bari, X. Correig and B. Bouchikhi, *Sensors*, 2008, **8**, 142–156.
31 Y.-K. Chung, M.-H. Kim, W.-S. Um, H.-S. Lee, J.-K. Song, S.-C. Choi, K.-M. Yi, M.-J. Lee and K.-W. Chung, *Sensors and Actuators B: Chemical*, 1999, **60**, 49–56.
32 J. Tamaki, *Sensor Letters*, 2005, **3**, 89–98.
33 W. Yu-De, C. Zhan-Xian, L. Yan-Feng, Z. Zhen-Lai and W. Xing-Hui, *Solid-State Electronics*, 2001, **45**, 639–644.
34 P. Varsani, A. Afonja, D. E. Williams, I. P. Parkin and R. Binions, *Sensors and Actuators B: Chemical*, 2011, **160**, 475–482.
35 W. H. Zhang, W. D. Zhang and L. Y. Chen, *Nanotechnology*, 2010, **21**, 315502.
36 S. N. Malchenko, Y. N. Lychkovsky and M. V. Baykov, *Sensors and Actuators B: Chemical*, 1993, **13**, 159–161.
37 A. Oprea, A. Gurlo, N. Bârsan and U. Weimar, *Sensors and Actuators B: Chemical*, 2009, **139**, 322–328.
38 V. Golovanov, M. A. Mäki-Jaskari, T. T. Rantala, G. Korotcenkov, V. Brinzari, A. Cornet and J. Morante, *Sensors and Actuators B: Chemical*, 2005, **106**, 563–571.
39 S. Elouali, L. G. Bloor, R. Binions, I. P. Parkin, C. J. Carmalt and J. A. Darr, *Langmuir*, 2011, **28**, 1879–1885.
40 G. N. Vayssilov, *Catalysis Reviews*, 1997, **39**, 209–251.
41 D. R. C. Huybrechts, P. L. Buskens and P. A. Jacobs, *Journal of Molecular Catalysis*, 1992, **71**, 129–147.
42 D. H. Olson, G. T. Kokotailo, S. L. Lawton and W. M. Meier, *The Journal of Physical Chemistry*, 1981, **85**, 2238–2243.
43 R. Millini, E. Previde Massara, G. Perego and G. Bellussi, *Journal of Catalysis*, 1992, **137**, 497–503.
44 J. Yinon and S. Zitrin, *Modern Methods and Applications in Analysis of Explosives*, John Wiley & Sons, Chichester, 1996, ch. 1.
45 J. R. Sohn, *Journal of Industrial and Engineering Chemistry*, 2002, **8**, 386–392.
46 L. Mazeina, F. K. Perkins, V. M. Bermudez, S. P. Arnold and S. M. Prokes, *Langmuir*, 2010, **26**, 13722–13726.
47 United Nations General Assembly, *Convention on the Marking of Plastic Explosives for the Purpose of Detection.*, Montreal, 1991.
48 H. Lee, G. Shaker, K. Naishadham, S. Xiaojuan, M. McKinley, B. Wagner and M. Tentzeris, *Microwave Theory and Techniques, IEEE Transactions on*, 2011, **59**, 2665–2673.
49 M. A. Uguina, D. P. Serrano, G. Ovejero, R. Van Grieken and M. Camacho, *Applied Catalysis A: General*, 1995, **124**, 391–408.
50 H. v. Koningsveld, J. C. Jansen and H. v. Bekkum, *Zeolites*, 1990, **10**, 235–242.
51 D. M. Ruthven, W. DeSisto and S. Higgins, *Chemical Engineering Science*, 2009, **64**, 3201 – 3203.